Hydrogen Interactions with a Pd₄ Cluster: Triplet and Singlet States and Transition Probability

Ernst D. German,* Irena Efremenko, and Moshe Sheintuch

Wolfson Department of Chemical Engineering, Technion—Israel Institute of Technology, Haifa 32000, Israel

The DFT method is used to analyze the singlet and triplet PES cross-sections for a number of reaction pathways of the interaction between a hydrogen molecule and a palladium tetramer. Stationary points characterizing stable singlet and triplet complexes and transition states are determined. Predissociated Pd_4H_2 complexes with binding energies of 5.0–6.4 kcal/mol are formed without an activation barrier at *any* initial orientation of reactants in the ground triplet state. The dissociated triplet complexes with adsorption energy of 4.7–8.4 kcal/mol are separated from the predissociated structures by the barrier of 11 kcal/mol. The dissociated singlet structures with hydrogen atoms located in two 3-fold positions and in the bridge positions on nonintersecting Pd–Pd bonds have the same binding energy of 22.1 kcal/mol and correspond to the ground state of the Pd_4H_2 system. Several more local minima corresponding to dissociated and nondissociated H–H bonds are found on the singlet PES. In contrast to the low-index bulk palladium surfaces, no spontaneous pathway for hydrogen dissociation on the cluster is found. Activated H_2 dissociation on the palladium tetramer includes the triplet–singlet transition induced by the spin–orbit interaction as a key step. Numerical estimation of the matrix spin–orbit coupling element and the corresponding transmission coefficient κ is performed within nonadiabatic theory for two reaction pathways, which are expected to have the maximal reaction probability. The estimated κ values of ~0.1 and ~0.4 and corresponding activation barriers of ~25 and ~20 kcal/mol are found for the reaction pathways leading to the ground-state three-coordinated dissociated complex and to the saddle point heading toward the ground-state bridge structure, respectively.

1. Introduction

Hydrogen activation by palladium catalysts has attracted significant attention because of its wide application in numerous industrial processes and as a well-suited model system for studying of different aspects relevant to catalysis. Recently, hydrogen dissociation on the low-index palladium surfaces was extensively studied by DFT methods using periodic model approximation.[1-4] In these calculations, the substrate was kept at the truncated bulk geometry with the calculated equilibrium lattice constant and the hydrogen molecular axis was kept parallel to the surface plane. The computations indicated that at least one reaction pathway for hydrogen dissociation with no or very low activation energy exists on each surface; yet, most hydrogen molecules with low kinetic energy are capped by palladium atoms and form weakly bound predissociated states. This theoretical result is in agreement with the molecular beam experiments.[5] Both thermodynamic and kinetic stability of the molecularly adsorbed complexes increases then moving from close-packed to more crystallographically "open" crystal faces. Further along the reaction coordinate, the adsorbed hydrogen molecule changes its position above the surface in the direction of the low potential pathway for dissociation ("steering" effect) followed by surface diffusion of separated H-atoms toward the final stable positions. Moreover, it was shown both experimentally[6] and theoretically[7] that H₂ approaching palladium, with the molecular axis being in the perpendicular direction to the surface, also leads to hydrogen dissociation with

direct absorption into the bulk. The surface relaxation is extremely important for this last reaction channel.

In contrast to the bulk surfaces, hydrogen activation on such perspective catalysts as small palladium clusters is significantly less studied. Alterations in the adsorbent geometry along the reaction pathway are likely to be more pronounced for small clusters than those for bulk surfaces. Moreover, there is strong evidence that, in variance to the single atom and bulk, small palladium clusters have an open-shell electronic configuration in the ground state.[8-23] These add complexity to the investigations of hydrogen interactions with cluster particles. Intensive high-level calculations of the potential energy surfaces (PES) and corresponding stable states for Pd_n-H_2 ($n = 1-4$) systems have been performed.[12-14,24-31] In some of these works,[25,26] palladium clusters served as a model of a bulk surface, where they had closed-shell electronic structure and geometry fixed at the *fcc* palladium crystalline lattice. In the other studies,[27-30] the cluster geometry was optimized for several highly symmetric adsorption positions. Full optimization of the geometry was done for Pd_n-H_2 systems with $n = 1-3$ in the DFT studies at the B3LYP level of theory for the several most stable stationary states.[12,13] The same method was applied for studying the precursor-mediated hydrogen dissociation on Pd_3 and Pd_4 clusters.[14] However, the results of such studies did not follow the whole reaction pathway from the ground-state reactants to the ground-state products and did not explain the dramatic differences in catalytic behavior of bulk palladium surfaces and small clusters observed experimentally.

The present work aims to find out the whole reaction pathways for hydrogen dissociation on small palladium clusters

* To whom correspondence should be addressed. Fax: 972-4-8230476. E-mail: cermsge@tx.technion.ac.il.

TABLE 1: Calculated Characteristics of the Hydrogen Molecule and of the Palladium Tetramer in the Singlet and Triplet States[a]

symmetry		C_{3v}		C_{2v}		C_s	
electronic state		singlet	triplet	(^{1}A$_1$)	(^{3}B$_1$)	(^{1}A′)	(^{3}A″)
Pd$_4$	d_{12}	2.651	2.604	2.846	2.606	2.852	2.603
	$d_{13} = d_{14}$	2.651	2.604	2.578	2.642	2.578	2.712
	d_{34}	2.652	2.714	2.846	2.782	2.845	2.721
	$d_{24} = d_{23}$	2.652	2.714	2.642	2.576	2.576	2.605
	E_t	−506.977636	−507.008530	−506.982386	−507.0081313	−506.982324	−507.008626
	ΔE	0	−19.4	−3.0	−19.1	−2.9	−19.4
H$_2$	E_t			−1.163650			
	d			0.7615			
	E_D			101.1			

[a] Reactants bond lengths are in angstroms, total energies E_t are in au, and relative energies ΔE and dissociation energy E_D are in kcal/mol. All energies include zero-point corrections. For notations of the geometrical characteristics, see Figure 1.

linking the ground states of reactants and products, which include the triplet−singlet transition as an essential constituent. The Pd$_4$ cluster is the simplest three-dimensional system of Pd atoms that may be used as a model of highly dispersed catalysts. Because the Pd$_4$−H$_2$ system has a flexible structure with numerous local minima, its theoretical study is not a trivial procedure. Furthermore, as it will be seen further, the reactants and products have different multiplicity in the ground electronic state. Therefore, the formation of the stable singlet complex from the triplet reactants, i.e., the dissociative adsorption of hydrogen on the palladium tetramer, as well as on other small palladium clusters, must proceed by a triplet−singlet transition that is an obligatory step of the reaction. In this spin-forbidden process, the minimum energy point on the intersection of two potential surfaces represents a key bottleneck along the minimum energy path (MEP), playing the same role as a transition state for an allowed reaction. However, to the best of our knowledge, this problem was not addressed in the published literature. The detailed investigation of the triplet and singlet PESs for various trajectories of the reactant approaches is the first necessary step related to this point.

In our previous paper,[31] we have studied certain stationary states for the Pd$_4$−H$_2$ adduct. In the present paper, we continue this work and report detailed calculation on the structure of the singlet and triplet potential surfaces of the system in comparison with the published DFT results for low-index bulk palladium surfaces.[1−4,7] The quantum chemical information about the PES structures obtained in these calculations is used then to evaluate the activation barriers and transition probabilities for several reaction pathways leading from the ground-state triplet reactants to the ground-state singlet products.

The paper is organized as follows. In section 2, the details of the computational method are presented. The singlet and triplet potential curves calculated for a number of approach modes of the reactants and the corresponding stationary states are discussed in section 3. Section 4 is devoted to the estimations of the spin−orbit matrix elements for two approach modes that are used to discuss the probability of the triplet−singlet transition. In Section 5, the obtained results are discussed in comparison with corresponding data for bulk low-index palladium surfaces and small clusters. Section 6 concludes.

2. Computation Details

The Pd$_4$/H$_2$ system is investigated by DFT method using the Gaussian 94 program.[32] We applied the B3LYP functional that involves the gradient correction of the exchange functional by Becke[33] and the correlational functional by Lee, Yang, and Parr.[34] The hydrogen was described in the cc-pVDZ basis set.[35]

For the Pd atom, the standard LANL2DZ basis, with 28 core electrons being replaced by the relativistic effective core potential (ECP) of Hay and Wadt,[36] was used. This basis was shown[12−14,16] to yield good results for Pd$_n$ clusters with n = 1−4. The cross-sections for a number of approach modes of hydrogen molecules toward the palladium cluster, that are the minimum energy paths (MEPs), are constructed as follows. A distance between Pd$_4$ and one of the H atoms or H$_2$ molecule center of mass is chosen as a variable, and other geometric parameters are optimized. The corresponding energy characteristic of a reaction between hydrogen and a palladium cluster is the quantity

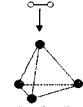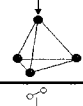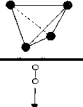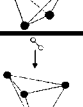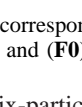$$\Delta E = E(\text{Pd}_4\text{H}_2) - E(\text{Pd}_4) - E(\text{H}_2) \quad (1)$$

where $E(\text{Pd}_4)$, $E(\text{H}_2)$, and $E(\text{Pd}_4\text{H}_2)$ are the total energies of reactants and products. For both multiplet states, ΔE is calculated with respect to the triplet state of the Pd$_4$ cluster under the same symmetry constraint as that applied for Pd$_4$H$_2$, unless otherwise specified. In a further discussion, the binding energy is characterized as $E_b = -\Delta E$ and the activation energy as $E_a = \Delta E$. All presented E_b values for stationary states include zero point corrections.

The structure and energetic characteristics of the free reactants, i.e., the palladium tetramer in the singlet and triplet electronic state and H$_2$ molecule, used to calculate the MEPs according to eq 1, are presented in Table 1. As in the case of the palladium dimer and trimer,[12,13,15−19] the Pd$_4$ cluster has the triplet multiplicity in the ground state, with C_{2v} and C_s symmetries being more stable than C_{3v} symmetry. The right tetrahedral Pd$_4$ clusters considered in ref 10 are not *real* minima on the potential surface in both spin states and show Jan-Teller distortion. For the H$_2$ molecule, the applied computational scheme overestimates the dissociation energy D_E by 2% and bond length d by 0.015 Å in comparison with the corresponding experimental values.[37]

**3. Triplet and Singlet PES Cross-Sections for H$_2$−Pd$_4$ Interactions**

Within the Born−Oppenheimer and rigid-substrate approximations, the PES for dissociative adsorption of hydrogen is a six-dimensional hypersurface. At present, its calculation is still a numerically prohibitive task for high-level quantum chemical methods. Thus, to study the hydrogen interactions with low-index bulk palladium surfaces, DFT methods were used for construction of some low-dimensional cuts, from which the high-dimensional PES can be built by interpolation.[1−4,7] In the present study, we applied the same approach for the flexible

TABLE 2: Summary of the Stable State Localized for All of the Studied Approach Modes

Approach modes	Molecular adsorption				Dissociative adsorption			
	Spin	E_b	Complex	Figure	Spin	E_b	Complex	Figure
Bond_top	1	6.2	(A1)	1,ii	1	4.7	(B1)	1,ii
	0	-11.3	(A0)	1,ii	0	21.7	(B0)	1,ii
Atom_top	No stable structure are found for such orientation. With allowed angular rotation this approach mode transforms into the bond_to_top one (scheme in Fig.1,i)							
Bond_bond	1	5.3	(D1)	4,ii	0	22.1[b]	(C0)	4,ii
	1	5.3[a]	(E1)	4,ii				
Atom_bond	With allowed translations transforms into the precursor state from the first row (scheme in Fig. 4,iii)				1	8.4	(F1)	4,iv
					0	22.1	(F0)	4,iv
Bond_face	1	6.4	(I1)	7,ii	0	11	(G0)	7,ii
					0	16.8	(H0)	7,ii
Atom_face	With allowed translations transforms into the precursor state from the first row (scheme in Fig. 7,iii)				0	22.0[c]	(J0)	7,iv

[a] The stable structures (E1) and (A1) correspond to the nearly degenerated states with similar geometries. [b] The same for the structures (C0) and (B0). [b] The same for the structures (J0) and (F0).

geometry of the adsorbent. For the six-particle system, the PES has 12 independent variables. To reduce the dimensionality, we impose C_s or C_{2v} symmetry constraints. The triplet and singlet PES cross-sections for the gas-phase reaction

$$Pd_4 + H_2 \rightarrow Pd_4H_2 \qquad (2)$$
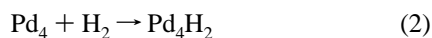
were calculated for the following approach modes of a hydrogen molecule toward the palladium cluster: (a) atom-to-top, atom-to-bond, and atom-to-face, if the H atom of the molecule attacks a top, a bond, or a face of the palladium tetramer and (b) bond-to-top, bond-to-bond, and bond-to-face, if the H–H bond attacks the same positions of the palladium cluster.

As in the case of bulk surfaces, these initial dispositions of the reactants present the boundary reaction pathways for the adsorbate approaching 1-, 2-, and 3-fold coordination positions at arbitrary orientation. For each orientation, the incident hydrogen molecule was first directed toward the top palladium atom or toward the center of a Pd–Pd bond. After that, the molecule was shifted according to the forces driving it into a local minimum. The results for the stable states identified as real minima on the potential surfaces for these approach modes are summarized in Table 2.

Below in this section, we discuss the MEPs leading to the formation of the presented stable Pd_4H_2 structures. Of the possible reaction pathways resulting in the ground state dissociated complexes, we chose the most energetically favorable ones and estimate the kinetic transition probability in the next section.

3.1. Atom-to-Top and Bond-to-Top Approach Modes. In the atom-to-top approach mode, first an incident H_2 molecule is located strictly on the perpendicular to the base of the Pd_4 pyramid passing through the top Pd atom. This approach mode is shown schematically as the (a1)/(a0) configuration in Figure 1i (numbers 1 and 0 indicate here and below the spin state of the system). In Figure 2, the MEP curves 1 and 2 demonstrate the energy changes along this reaction pathway in the ground triplet and excited singlet states of the system, respectively. In the whole region of s values, the triplet state remains about 16.5 kcal/mol lower. Analysis of the normal vibrations shows that the shallow minima at $s \sim 2.1$ Å in these curves do not characterize true stable states. If the hydrogen molecule is allowed to rotate around its center of mass (Figure 1i and curve 3 in Figure 2), the optimized angle φ increases as the palladium cluster is approached and reaches 90° at the stationary point (b1) in Figures 1i and 2. This parallel orientation of the hydrogen molecule (bond-to-top mode) is more energetically advantageous than the perpendicular one; nevertheless, the stationary point (b1) still does not describe a true minimum on the PES. It presents a transition state that, following the imaginary mode in the corresponding set of the normal frequencies, transforms into the stable structures (A1) and (A0) shown in Figure 1,i,ii.

Figure 3i displays the triplet and singlet PES cross-sections obtained for the bond-to-top approach mode under the C_s symmetry constraint with fixed parameter $b = 0$ ((b0) and (b1) configurations in Figure 1i). Computational difficulties arising from the symmetry constraint hamper calculation of these MEP curves in the range of x values between 2.4 and 3.5 Å. It is important to note that the triplet state is significantly lower at large distances between the reactants, whereas at small distances of x characteristic for a broken H–H bond, the inversion of the stability of triplet and singlet states occurs. In the stationary points (b1) and (b0) located at $x = 4.076$ and 4.104 Å in the triplet and singlet curves, respectively, the H–H bond is only

Hydrogen Interactions with a Pd$_4$ Cluster

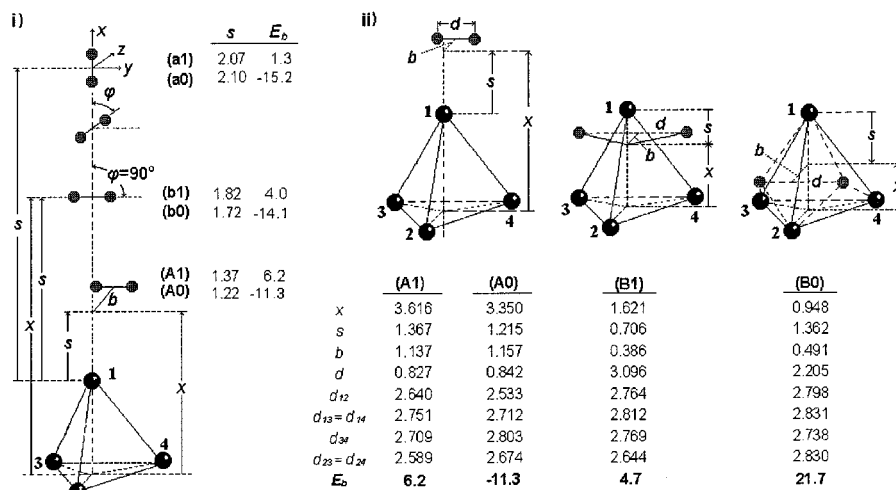*J. Phys. Chem. A, Vol. 105, No. 50, 2001* **11315**

Figure 1. Mutual arrangement of reactants (i) and stable structures (ii) localized in the atom-to-top and bond-to-top approach modes. The binding energies (E_b, kcal/mol) are presented for all of the stationary points shown in Figures 2 and 3,, whereas the geometric structures (in angstroms) are presented only for the stable states identified in Figure 3,ii. The large black spheres show Pd atoms, and small open circles stand for H atoms. The presented structures and the corresponding stationary points in the PES cross-sections are labeled with the same capital letters; the accompanying numbers show the multiplicity.
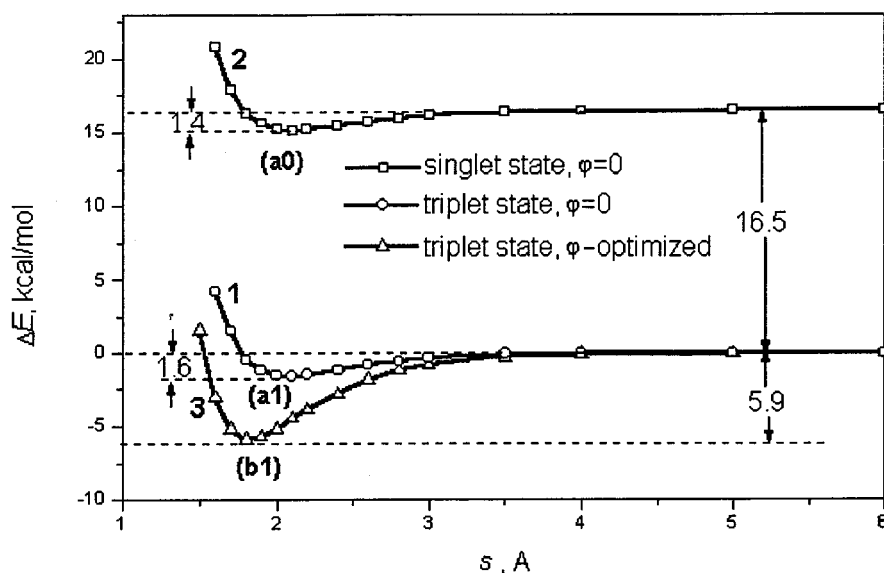

Figure 2. Triplet and singlet MEP curves for the Pd$_4$H$_2$ system in the atom-to-top approach mode calculated under C_s symmetry constraint at fixed (curves 1 and 2) and optimized (curve 3) angle φ. See Figure 1 for notations.

slightly elongated, with the former state lying significantly lower. In the stationary points at $x = 1.5$ and 1.036 Å, the hydrogen molecule is dissociated and the singlet state of the system becomes much more stable. As we will see below, the similar spin transition takes place for all considered reaction pathways.

The stationary points in Figure 3i do not describe true minima on the potential surfaces; however, according to the calculated normal vibrations, they transform into the corresponding stable states if an additional variable b is optimized (structures (**A1**) and (**A0**) in Figure 1,i,ii). The corresponding MEP curves are presented in Figure 3ii. In the triplet curve, the stationary point (**A1**) at $x = 3.62$ Å, into which the system spontaneously falls under the approaching of the reactants, indeed describes *true* stable structure. The *true* minimum (**A0**) at $x = 3.35$ Å in the singlet curve of Figure 3ii depicts an excited state that is destabilized by $\sim$11 kcal/mol as compared to the triplet reactants. In these complexes, the H−H bond length is elongated by $\sim$10−15% and the configuration of the Pd$_4$ fragment is only

slightly disturbed in comparison with the free reactants. These two structures were presented in ref 14, with the geometric and energetic characteristics being very close to those shown in Figure 1ii for the structures (**A1**) and (**A0**). The energetic and geometric results presented in Figure 1i together with PES cross-sections from Figures 2 and 3 demonstrate that in the ground electronic state at low kinetic energy a hydrogen molecule approaching a vertex of a Pd$_4$ pyramid is rotated and shifted until the weakly bound molecular complex (**A1**) is formed. For any orientation of an incident molecule, the process goes with continuous energy gain.

Now let us discuss the range of x values below the intersection of the singlet and triplet curves ($\sim$2.2 Å; Figure 3ii). The stationary point (**B1**) at $x \sim 1.6$ Å in the triplet curve is $\sim$ 17 kcal/mol higher than the corresponding point (**B0**) in the singlet curve. The triplet minimum (**B1**) characterizes the true stable structure with the geometry shown in Figure 1ii, but it is destabilized by 1.5 kcal/mol as compared to the triplet molecular complex (**A1**). The H−H bond is completely broken in this
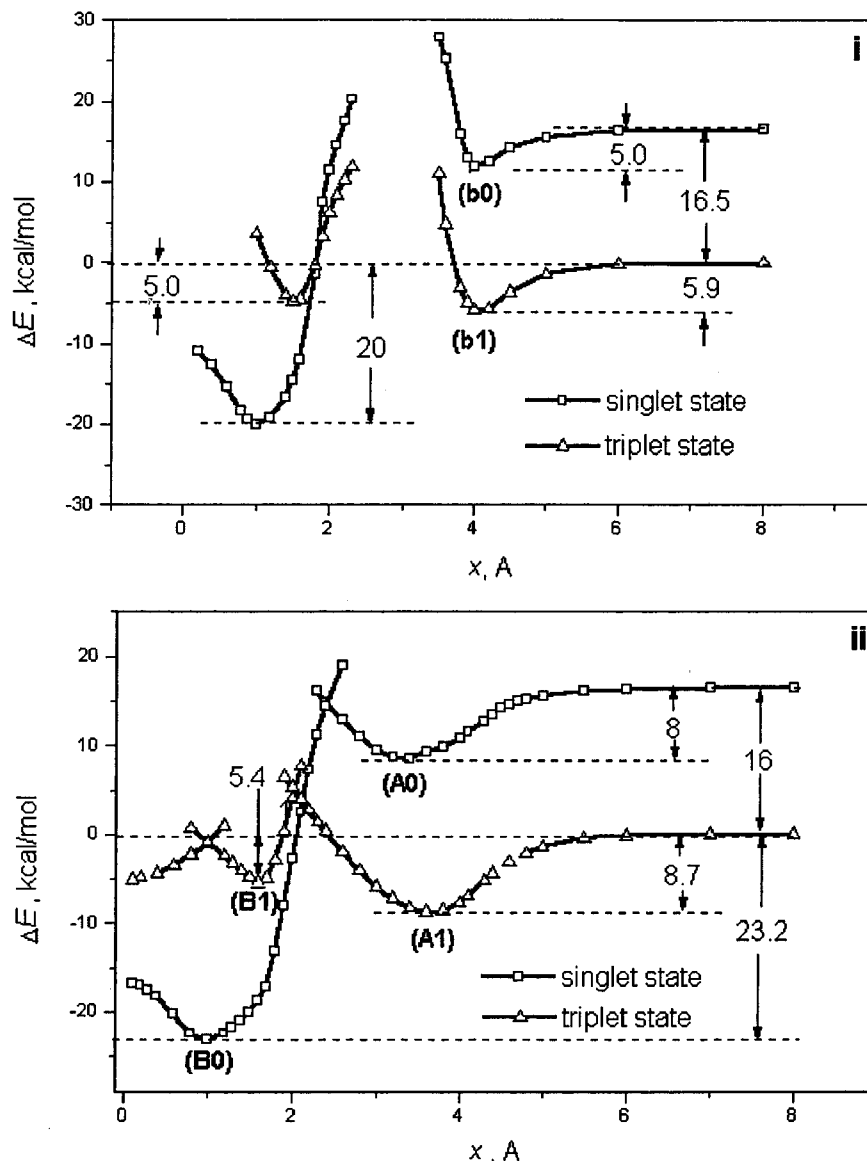
Figure 3. Triplet and singlet minimum energy paths for the Pd_4H_2 system in the bond-to-top approach mode calculated under C_s symmetry constraint with the fixed at zero (i) and optimized (ii) parameter b (see Figure 1,i; structures b and A, respectively).

stable complex. A transition state between the minima in the triplet curve cannot be found under the C_s symmetry constraint. However, if the symmetry is allowed to reduce, the corresponding transition state can be located about 3.6 kcal/mol above the energy of the triplet reactants that provides the activation barrier for the transition from (**A1**) to (**B1**) of ∼11 kcal/mol. The corresponding reaction pathway is described in detail in ref 14. Thus, on the triplet PES cross-section, the hydrogen dissociation on the Pd_4 cluster is energetically unfavorable as compared to that of the physisorbed state. In the approach mode under discussion, the most stable state of the Pd_4H_2 system presents the singlet complex (**B0**) with a completely dissociated H−H bond (Figure 1ii). This structure is characterized by the binding energy of 21.7 kcal/mol. Each H atom in this complex is bound to three palladium atoms. The reaction pathway for the formation of this stable complex on the singlet PES is also well described in ref 14. The authors found an activation barrier of 4.2 kcal/mol to hydrogen dissociation from the molecularly adsorbed state (**A0**). However, on the basis of the results of this work, nothing can be learned about the transition from the initial triplet into the final singlet state because the geometric structures of the singlet and triplet complexes in the crossing point of the

two potential surfaces differ dramatically. In the next section, we will apply the results presented above for estimation of the kinetic parameters of the process for the transition of ground-state triplet reactants to ground-state singlet products.

3.2. Bond-to-Bond and Atom-to-Bond Approach Modes. The first approach mode of the reactants, considered in this subsection, has C_{2v} symmetry. In this reactant arrangement, a hydrogen molecule is located in the plane perpendicular to the C_{2v} symmetry axis of the cluster, with the H−H bond being perpendicular to the Pd_3−Pd_4 bond (scheme **a** in Figure 4i). The triplet and singlet MEP curves calculated under these constraints are shown in Figure 5i. Similar to the results obtained in the previous section, the triplet state of the system is more stable than the singlet state at large distances x between the reactants and it becomes much higher in energy at small distances x when the H−H bond is dissociated. The triplet curve consists of a number of branches, and their crossing points characterize sharp changes in the structure of the complex. The stationary points found in the triplet curve at $x \sim 1.8$ and ∼2.7 Å do not correspond to true minima on the PES. The singlet curve includes two branches corresponding to the nondissociated and dissociated H−H bond. The stationary point in the left
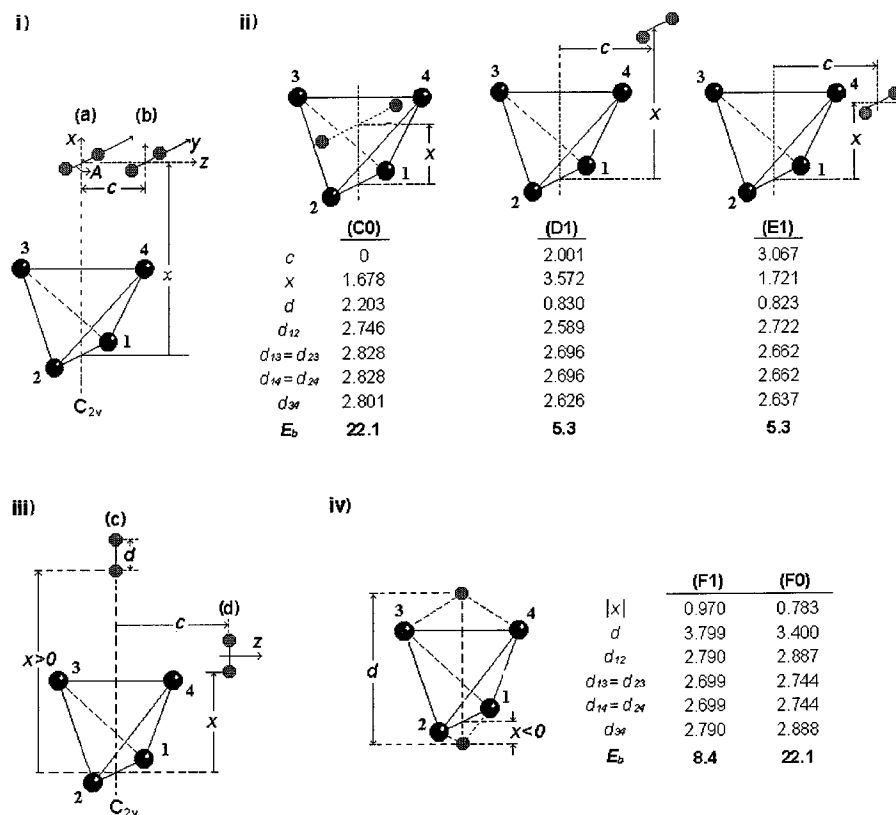
Hydrogen Interactions with a Pd$_4$ Cluster

J. Phys. Chem. A, Vol. 105, No. 50, 2001 **11317**

	(C0)	(D1)	(E1)
c	0	2.001	3.067
x	1.678	3.572	1.721
d	2.203	0.830	0.823
d_{12}	2.746	2.589	2.722
$d_{13}=d_{23}$	2.828	2.696	2.662
$d_{14}=d_{24}$	2.828	2.696	2.662
d_{34}	2.801	2.626	2.637
E_b	22.1	5.3	5.3

	(F1)	(F0)
$|x|$	0.970	0.783
d	3.799	3.400
d_{12}	2.790	2.887
$d_{13}=d_{23}$	2.699	2.744
$d_{14}=d_{24}$	2.699	2.744
d_{34}	2.790	2.888
E_b	8.4	22.1

Figure 4. Mutual orientations of reactants (i and iii) and stable Pd$_4$H$_2$ complexes (ii and iv) localized in the bond-to-bond (i and ii) and atom-to-bond (iii and iv) approach modes. The structural data are given in angstroms, and the binding energies are in kcal/mol.

branch of the curve characterizes the *true* stable structure (**C0**) shown in Figure 4ii. This structure coincides with the structure (**B0**) (Figure 1ii) localized in the bond-to-top approach mode; the geometries and energies of these two complexes, however, differ somewhat. These two complexes present the striking example of the existence of numerous nearly degenerated states with similar structures even in such a small system as Pd$_4$H$_2$. It is interesting to note that the higher symmetry complex has a slightly lower energy.

As it follows from Figure 5i, the interaction of the triplet reactants in the symmetric configuration shown in Figure 4i has a repulsive character. The repulsion becomes weaker and then changes to an attraction if the incident hydrogen molecule is shifted from the center of attacked Pd$-$Pd bond by a parameter c (scheme **b** in Figure 4i). The corresponding MEP curves calculated for several fixed and for optimized variable c are presented in Figure 5ii. Two stationary points localized in the latter case at $x = 3.57$ and 1.72 Å correspond to the *true* stable structures (**D1**) and (**E1**), with the same binding energy of 5.3 kcal/mol (Figure 4ii.). The latter complex coincides with the structure (**A1**) in Figure 1i, with diminutive geometric and energetic differences originating from the applied symmetry constraints. A very small barrier separates two minima (**D1**) and (**E1**), so that their mutual transitions could proceed with the considerable rate. In other words, the molecularly adsorbed state is obviously distributed in almost equal proportion between these two structures. On the contrary, in the singlet state, the incident hydrogen molecule prefers the symmetric position, with its center of mass being on the C_{2v} axis ($c = 0$).

The effect of hydrogen rotation by angle A in the plane perpendicular to the C_{2v} symmetry axis (scheme **a** in Figure 4i) on the form of the triplet MEP curve has been studied for the particular case of $c = 0$. Obtained results (Figure 5iii) indicate that the perpendicular orientation of incoming hydrogen

molecules toward the attacked Pd$-$Pd bond ($A = 90°$) is somewhat more favorable than other arrangements including the parallel orientation of Pd$-$Pd and H$-$H bonds. However, the energy difference between the boundary orientations is very small (about 0.6 kcal/mol at x down to $\sim$ 3.6 Å). Therefore, the hydrogen molecule tends to arrange perpendicular to the nearest Pd$-$Pd bond and to shift toward one of the Pd atoms of the bond. As we have seen above, this pathway results in the triplet predissociated Pd$_4$H$_2$ complex.

Now, let us consider the end-on orientation of H$_2$ along the C_{2v} symmetry axis toward the approaching Pd$-$Pd bond (atom-to-bond approach mode; scheme **c** in Figure 4iii). The corresponding triplet and singlet potential curves are presented in Figure 6i. The approach of the reactants in this mode is characterized by a significant repulsion in the entrance channel, especially on the triplet PES. The stationary points localized on the left branches of these curves correspond to the stable structures (**F1**) and (**F0**) shown in Figure 4iv and present probably the global minima on the triplet and singlet potential surfaces, respectively. Two hydrogen atoms in these complexes are bound to nonintersecting Pd$-$Pd bonds, and their structures and energetics are very consistent with the previously obtained results.[13,14] The crossing point of the triplet and singlet curves at $x \sim 2.2$ Å lies $\sim$20 kcal/mol above the initial state. However, the geometric structures of the triplet and singlet Pd$_4$H$_2$ complexes at the crossing point differ significantly. Therefore, geometric transitions will further give rise to the activation barrier to hydrogen dissociation accompanied by intersystem crossing. That allows us to expect a very high activation barrier for the given approaching trajectory and to consider this reaction pathway as unfavorable for the hydrogen dissociation. So, the formation of the structure (**F0**) which is the most stable one in the Pd$_4-$H$_2$ system is assumed to proceed by a two-stage or
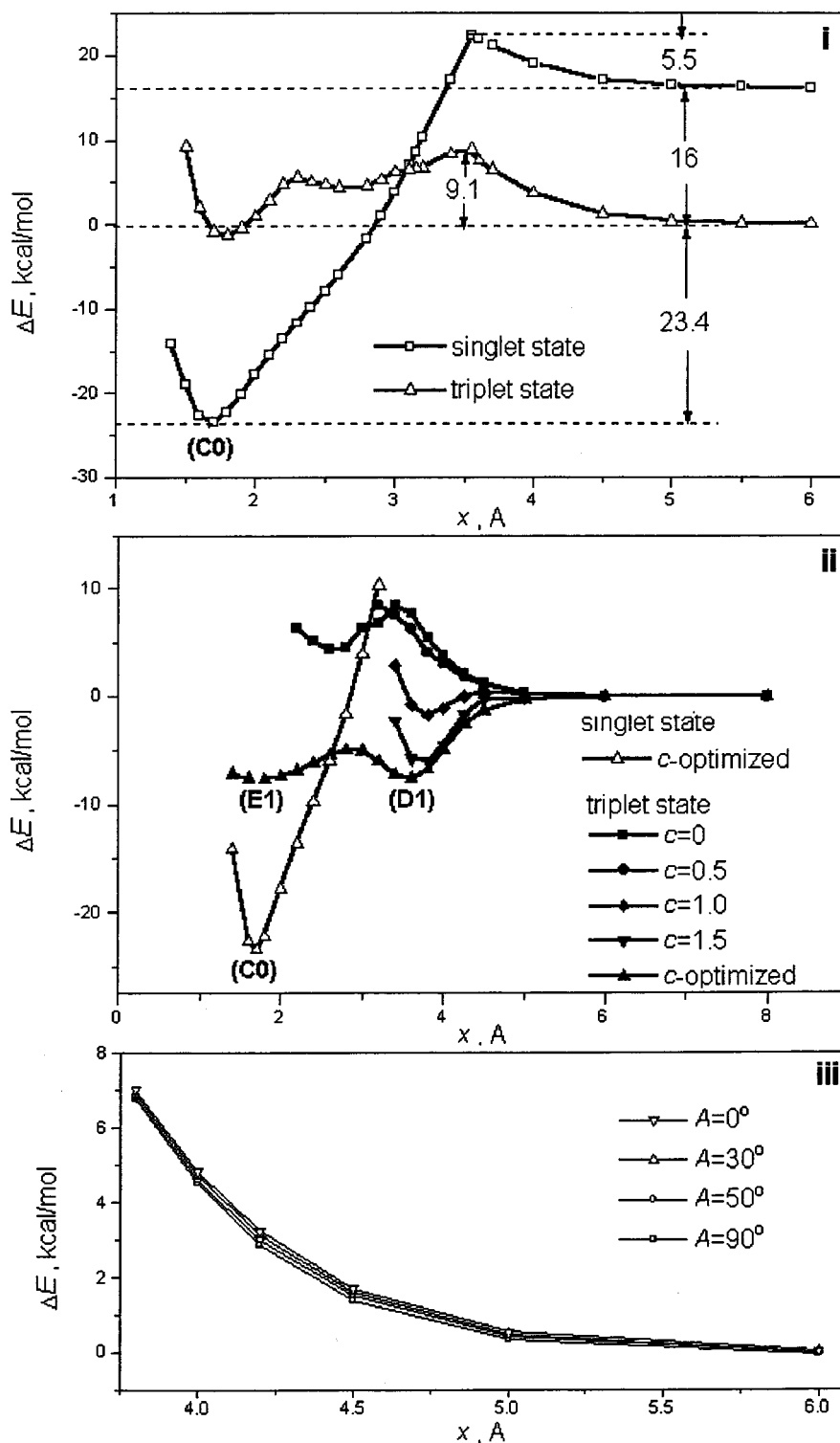
Figure 5. MEP curves for bond-to-bond approach mode calculated for $\angle A = 90°$ (perpendicular orientation of the H−H and the nearest Pd−Pd bonds), $c = 0$ (i); $\angle A = 90°$, c − variable (ii); and $\angle A$ − variable, $c = 0$ (iii).

more complex process (see the next section) but not as a result of the interaction of reactants along this highly symmetric pathway.

Indeed, the situation considerably changes if the symmetry is reduced and the hydrogen molecule is allowed to shift in parallel to the attacked Pd−Pd bond at the distance c (scheme **d** in Figure 4iii). The triplet PES cross-sections for such an approach of H$_2$ molecules toward the Pd$_4$ cluster calculated at several fixed c values and with the parameter c included in the

optimization procedure are shown in Figure 6ii. The repulsion becomes weaker with increasing c and is replaced by an attraction if the parameter c is optimized. It should be noted, however, that the stationary point in curve 6 at $x \sim 1.8$ Å is not a true minimum on the PES. Forces move this structure to the weakly bound molecular complexes shown in Figures 1ii and 4ii. Thus, the attack of a palladium cluster by a hydrogen molecule in the atom-to-bond approach mode does not lead to the hydrogen dissociation. Again, the molecule is steering to
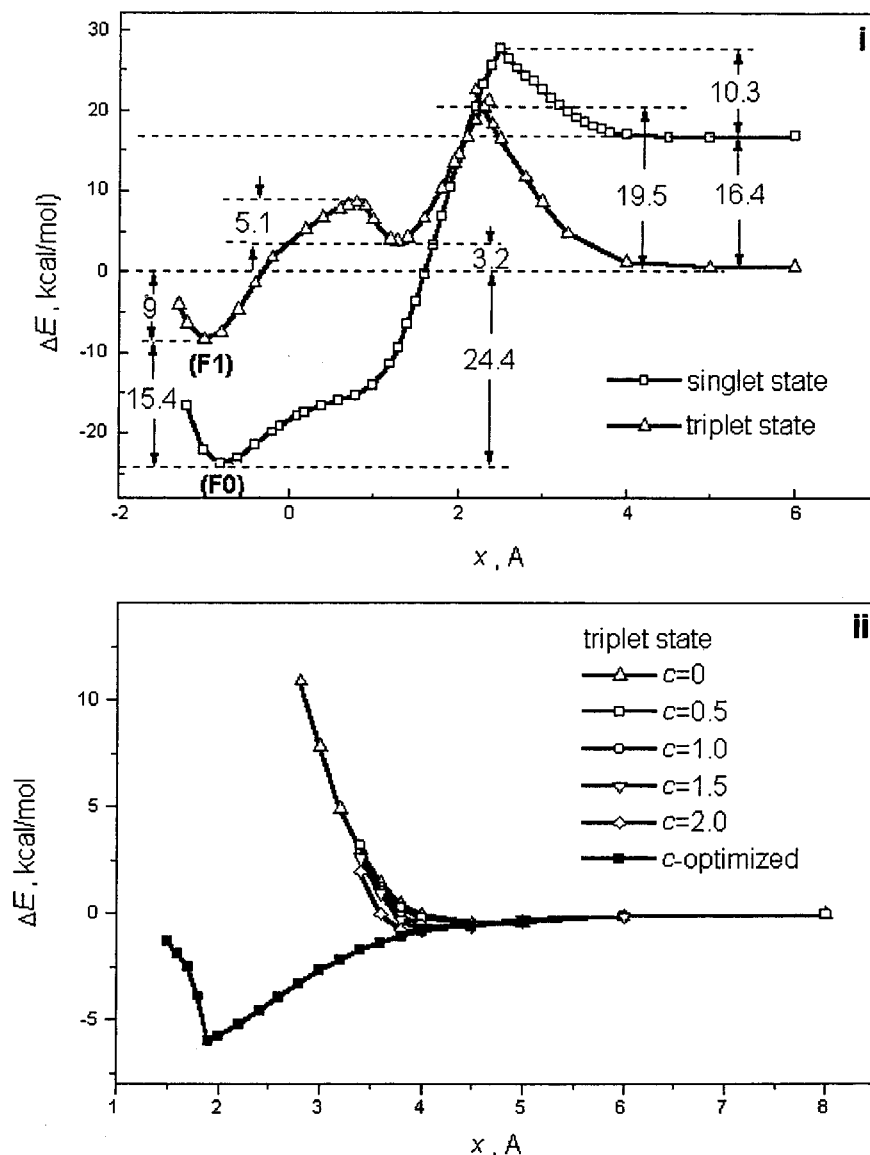
Hydrogen Interactions with a Pd$_4$ Cluster

J. Phys. Chem. A, Vol. 105, No. 50, 2001 **11319**

Figure 6. MEP curves for the atom-to-bond approach mode calculated for the fixed $c = 0$ (i) and for the variable parameter c (ii).

the molecular adsorptive complex with H$_2$ bound to one of palladium atoms and shifted slightly from the attitude of Pd$_4$ pyramid.

The atom-to-bond and bond-to-bond modes present the extreme orientations, which describe the angular rotation of a hydrogen molecule approaching a Pd—Pd bond of the Pd$_4$ cluster (cp. Figure 4 parts i and iii). The comparison of the triplet MEP curves obtained for these modes at the fixed $c = 0$ (Figures 5i and 6i) demonstrates that at large x distances the repulsion of the reactants in the bond-to-bond approach mode is stronger than that in the atom-to-bond mode. However, in the atom-to-bond mode, the repulsion sharply increases at shorter distances between the reactants. On the contrary, if the H$_2$ molecule is allowed to shift along the nearest Pd—Pd bond at the optimized distance c (Figures 5ii and 6ii), the bond-to-bond mode becomes essentially more energetically preferable than the atom-to-bond mode. Furthermore, our calculations show that the rotation of the hydrogen molecule resulting in a transition from the atom-to-bond to the bond-to-bond mode proceeds without an activation barrier at $x < 4$ Å. Thus, at low kinetic energy, the attack of a Pd—Pd bond on the ground-state triplet Pd$_4$ cluster by a hydrogen molecule in any orientation leads to the nonactivated steering of the hydrogen molecule to one of the Pd atoms with

formation of the molecular complexes. These complexes are very similar to those found in the case of H$_2$ approaching toward one of the palladium atoms. Further transformation of the system from the nondissociated into the final dissociated state involves a transition between the triplet and singlet curves and will be discussed in the next section.

3.3. Bond-to-Face and Atom-to-Face Approach Modes. In this subsection, the results of the MEP calculations are given for H$_2$ approaching a face of the Pd$_4$ tetrahedron (3-fold coordination site) with the endmost parallel and perpendicular orientations referred to as bond-to-face (Figure 7i) and atom-to-face (Figure 7iii) modes, respectively. Movement of the hydrogen molecule in the bond-to-face approach mode is restricted so that the H—H bond is parallel to the Pd(3)—Pd(4) bond of the cluster. First, we shall consider a particular geometry of the system, with the hydrogen center of mass being placed at the extension of the attitude of the Pd$_4$ pyramid (scheme **a** in Figure 7i). The corresponding triplet and singlet potential curves are shown in Figure 8i. The stationary point in the exit channel of the singlet curve corresponds to the *true* stable dissociated structure (**G0**), with the geometric and energetic parameters given in Figure 7ii. In the triplet state, similar to the symmetric atom-to-bond mode (Figure 4iii), the approaching of reactants
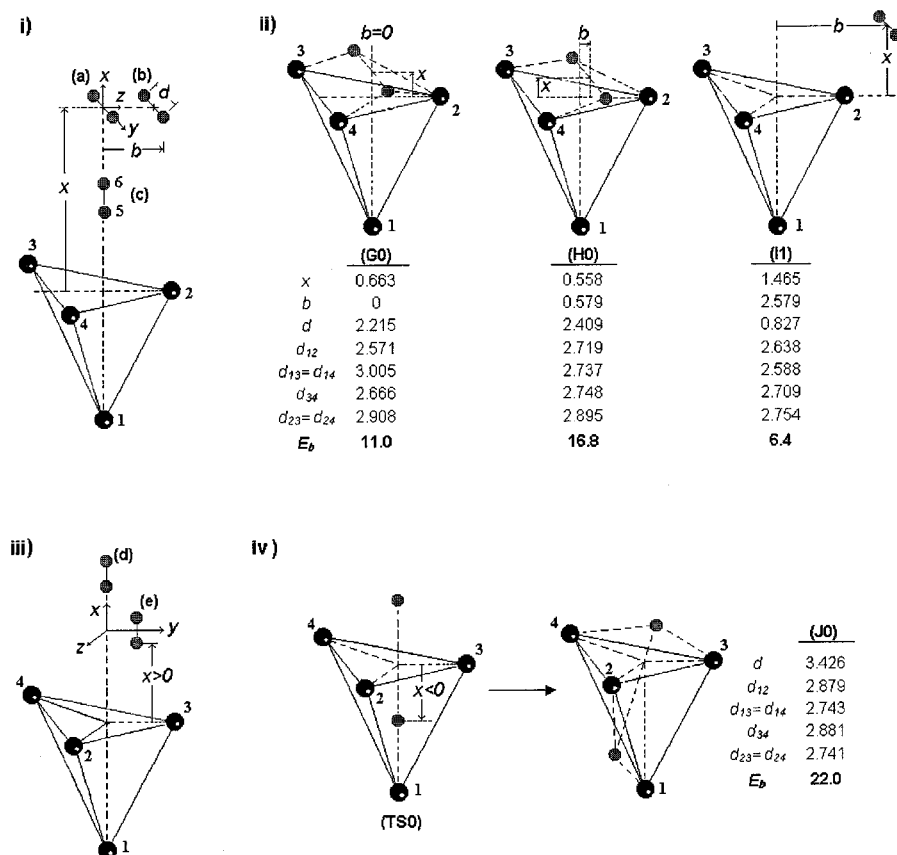
Figure 7. Mutual orientations of reactants (i and iii) and stable Pd_4H_2 complexes (ii and iv) arranged in the bond-to-face (i and ii) and atom-to-face (iii and iv) approach modes.

is accompanied by a significant repulsion, and at the crossing point, the geometric characteristics of the system in the two spin states differ considerably. Therefore, one may assume that, as in the case of the symmetric atom-to-bond mode, the formation of the final singlet product along this reaction pathway requires surmounting a high barrier.

The stationary point at $x \sim 0.5$ Å in the triplet curve (Figure 8i) is the transition state, in which forces shift the H_2 molecule on some distance b in the yz plane (scheme **b** in Figure 7i). The parameter b has a remarkable effect on the form of the triplet curve (Figure 8ii). The stationary point at $x =1.465$ Å localized under the optimized b variable describes the *true* stable complex (**I1**) (Figure 7ii). This complex has about the same geometry and binding energy as complex (**A1**) (Figure 1ii) found in the bond-to-top approach mode (Figure 3ii). In the singlet state, the optimization of the parameter b yields the complex (**H0**) (Figure 7ii). Its geometry slightly differs from that of the complex (**G0**); the corresponding binding energy is ~ 6 kcal/mol higher, and its formation is accompanied by the minor change in the form of potential curve at $x < 1.5$ Å.

The atom-to-face approach mode (Figure 7iii) is the last one considered in the paper. The triplet and singlet MEP curves calculated under the C_s symmetry constraint for the entrance and exit channels are presented in Figure 9. Stationary points in the triplet and singlet curves do not belong to true stable structures, as it follows from their normal vibrations. However, in the singlet curve, the stationary point (**TS0**) at $x = -1$ Å with the binding energy of about 12.7 kcal/mol presents the transition state, which transforms into the stable complex (**J0**) (Figure 7iv) when moving along a normal coordinate associated with the imaginary vibration. The latter structure corresponds with the complex (**F0**) (Figures 4iv and 6i) and presents the ground state of the Pd_4-H_2 system. Thus, the transition state

(**TS0**) accords the way for the direct formation of the ground-state product with reasonable activation energy. The activation barrier for the formation of the singlet product from the triplet reactants is determined by a position of the crossing point between the triplet and singlet curves located at $x \sim 0.8$ Å (Figure 9). This particular point is indeed the saddle where the structure of the Pd_4H_2 complex is practically the same in both of the spin states. The transition from the triplet reactants to the singlet product might occur with a maximum probability near this point (see below). Therefore, the activation energy of the dissociative hydrogen adsorption on the Pd_4 cluster in this mode is estimated as about ~ 25 kcal/mol.

Such a reaction pathway for hydrogen dissociation is probably effective at high kinetic energy. If the hydrogen molecule is allowed to shift at distance b out of the extension of the attitude of the Pd_4 pyramid and to rotate around the z axis (scheme **e** Figure 7iii), we come back to the formation of weakly bound molecular complexes described above. As in the previous cases, this latter reaction pathway will dominate if the hydrogen molecule approaches the 3-fold position of the palladium cluster at low kinetic energy. The subsequent transformation of this triplet complex into the final singlet product with a dissociated H−H bond is discussed in the next section.

4. Triplet−Singlet Transition Probability

The most salient feature of hydrogen interactions with palladium clusters, which distinguishes them from bulk surfaces, is that the dissociative interaction of hydrogen and the Pd_4 cluster is a spin-forbidden process. It involves the transition from the initial triplet state of the system into the final singlet state. This fact has been mentioned in the literature[13,14] and follows from the above detailed calculations on the Pd_4-H_2 system.

Hydrogen Interactions with a Pd$_4$ Cluster

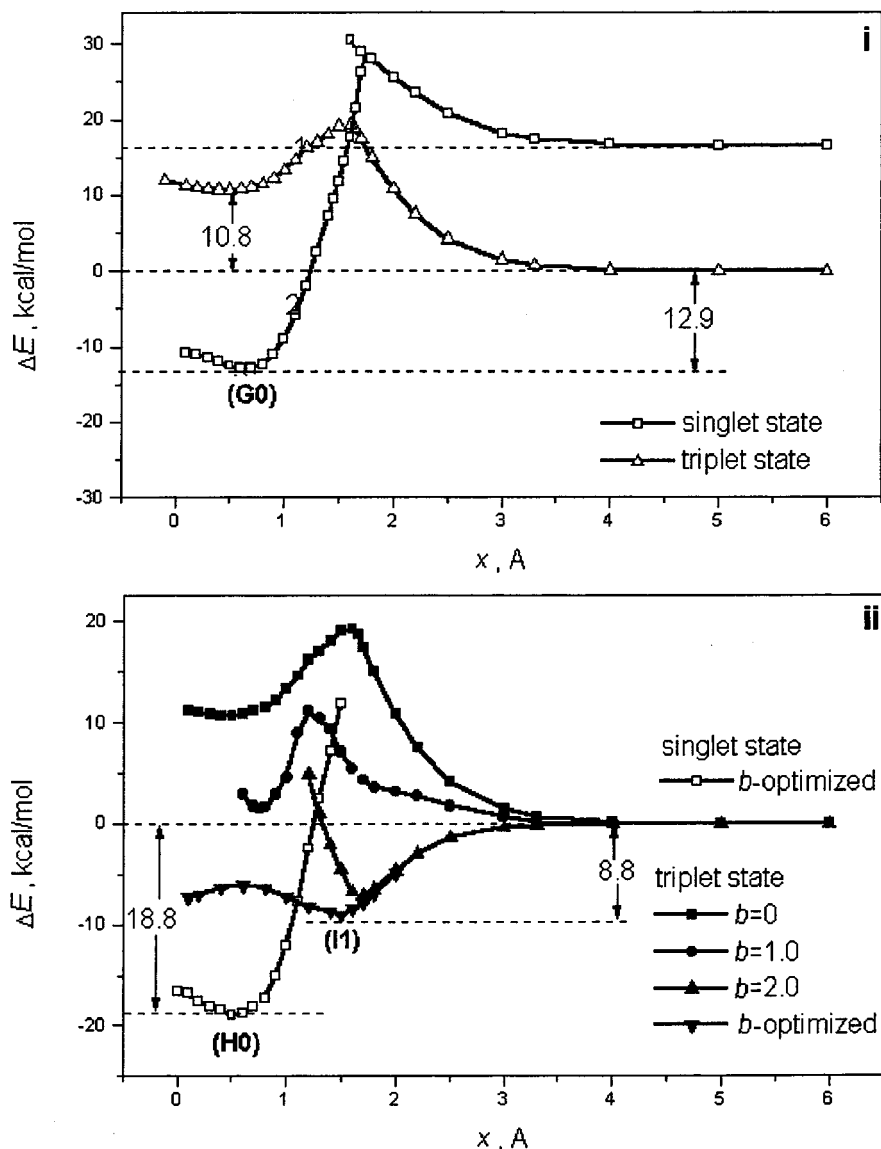*J. Phys. Chem. A, Vol. 105, No. 50, 2001* **11321**

Figure 8. MEP curves for the bond-to-face approach mode calculated under the C_s symmetry constraint with the fixed at zero (i) and optimized (ii) parameter b (see Figure 7,i; schemes **a** and **b**, respectively).

Estimation of the transition probability is of special interest because it provides an evaluation of the preexponential factor. The triplet−singlet transition might proceed through the spin−orbit coupling since the corresponding operator V_{LS} mixes different spin states. The estimation of this probability along with the direct data based on the calculations of the form of the potential energy surface of the system for various approach directions of the reactants might give additional information about the character of the considered reaction.

According to the Franck−Condon principle,[38] the maximal probability of the electron reorganization under the triplet−singlet transition occurs in the region near the saddle point on the crossing line of the triplet and singlet many-dimensional surfaces, where the coordinates of nuclei are the same in the both electronic states. In terms of the theory of nonadiabatic chemical reactions, this principle leads to the following expression for the total reaction probability:[39]

$$W = \frac{\omega_{\text{eff}}}{2\pi} \kappa \exp[-E_a/k_B T] \qquad (3)$$

where ω_{eff} is the effective frequency for the motion of nuclei,

κ is the electronic transmission coefficient, and E_a is the activation energy estimated as the energy difference between reactants and the minimum energy point on the intersection of singlet and triplet potential surfaces. According to eq 3, the total reaction probability W involves two factors. One of them characterizes the probability to reach the saddle point in which the triplet and the singlet states of the system are equal in energy. The second factor (transmission coefficient) determines the probability of the rearrangement of the triplet electronic state of the system into the singlet electronic state. For a nonadiabatic reaction, the electronic transmission coefficient may be approximately written as

$$\kappa \sim V_{\text{ts}}^2/V_{\text{cr}}^2 \qquad (4)$$

where V_{ts} is the matrix element of the spin−orbit interaction calculated at the saddle point and V_{cr} is its critical value. Typical values of ω_{eff} are $k_B T/\hbar \sim 10^{13}$ s^{-1}.[39]

In the Condon approximation,[38] the matrix element can be written as follows:

$$V_{\text{ts}} = \langle \varphi^{\text{T}}(\{r_\kappa\})|V_{\text{LS}}|\varphi^{\text{S}}(\{r_\kappa\})\rangle \qquad (5)$$
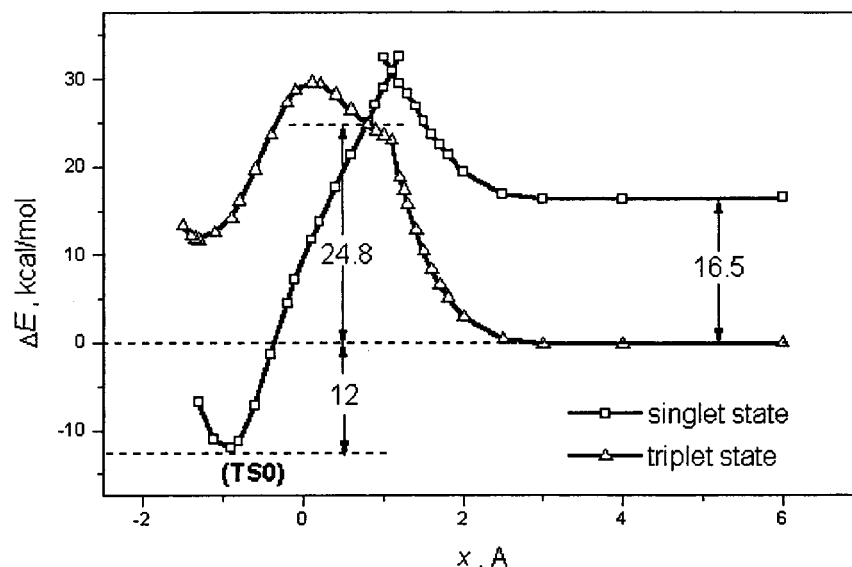
Figure 9. MEP curves for the atom-to-face approach mode (Figure 7,iii; scheme **d**).

where $\varphi^T(\{r_\kappa\})$ and $\varphi^S(\{r_\kappa\})$ are the triplet and singlet many electron wave functions of the Pd_nH_2 system in the transition configuration. This particular form can be used because the singlet and triplet functions are orthogonal because of the orthogonality of the spin functions. A more general expression for the matrix element may be found, for example, in ref 38.

In general, the spin−orbit operator may be written[40] as the sum of one-electron and two-electron terms, i.e.

$$V_{LS} = \sum_\mu [\sum_{k=1}^N h_{SO}^{(1)}(\mu; k) + \sum_{k<l}^N h_{SO}^{(2)}(\mu; k, l)] \quad (6)$$

where k and l numerate electrons and μ numerates nuclei. The first term in eq 6 describes the coupling between the spin magnetic moment of electron k and the effective magnetic field acting on it due to its motion in the electrostatic field of nucleus. The second term describes analogous electron−electron interaction.

One- and two-electron spin−orbit integrals in eq 6 can be evaluated directly or expressed through a linear combination of nuclear attraction and electron-repulsion integrals, respectively.[40] We shall restrict ourselves by an approximate consideration of the spin−orbit interaction for the system under consideration. Let us take advantage of ZDO approximation[41] and use the corresponding orbital transformation method.[42−43] We note that all integrals of two-electron operators in eq 6 vanish in the ZDO approximation.[42] Neglecting the two-electron component in the spin−orbit operator seems to be justified for our estimation of the triplet−singlet transition. Indeed, the computation of the contribution of the two-electron matrix elements into the spin−orbit interaction for a PdCl molecule made in ref 47 (the authors thank the referee who attracted our attention to this work) shows that it amounts to about 20−25% of the one-electron component being opposite in sign. The two-electron contribution in the Pd_4/H_2 system is believed to be of the same order of magnitude. Therefore, the one-electron component will provide us the upper limit of the spin−orbit interaction. The one-electron operators in eq 6 are equal to[44]

$$h_{SO}^{(1)}(\mu,1) = \xi_1(\vec{r}_{\mu,1})\vec{l}_{\mu,1}\cdot\vec{s}_1 \quad (7)$$

where $\vec{l}_{\mu,1}$ is the orbital angular momentum of an electron 1 with respect to the center of the μth atom. Equation 7 describes

the coupling between the spin magnetic moment of electron 1 and the effective magnetic field due to its motion in the electrostatic field of nucleus μ. Then, the electron matrix element (5) can be presented in the form

$$V_{ts} \equiv (V_{LS})_{fi} = \sum_\mu \langle \psi_N^S(1)\alpha|\xi_1(\vec{r}_{\mu,1})\vec{l}_{\mu,1}\cdot\vec{s}_1|\psi_N^T(1)\beta \rangle$$

$$= \frac{1}{2}\sum_\mu \langle \psi_N^S(1)|\xi_1(\vec{r}_{\mu,1})\cdot(\vec{l}_-)_{\mu,1}|\psi_N^T(1)\rangle \quad (8)$$

where ψ_N^T and ψ_N^S are the highest half-occupied molecular orbital in the triplet state and the highest occupied molecular orbital in the singlet state, and $\hat{l}_-$ is the orbital moment operator of translation. Here, we neglected the relaxation of the inner molecular orbitals in the triplet state as compared to the singlet state. Because the orbital moment of the H atom is zero in the ground state, the spin−orbit constant ξ in eq 8 is that for 4d electrons of the palladium atom, ξ_{4d}. Therefore, the summation in eq 8 can be performed only over palladium atoms. Moreover, at small distances from a nucleus, the spin−orbit constant $\xi(\vec{r})$ decreases rapidly and approaches zero as $1/r^3$.[44]

This fact allows approximate representation of the spin−orbit interaction for the many-atom system in terms of interactions on individual atoms by considering the atoms as independent centers. Therefore, eq 8 may be rewritten as follows:

$$V_{ts} = [\xi_{4d}(Pd)/2](\sum_{j=1}^4 \sum_{\substack{l=0,1,\\-1,-2}} (c_t)_l^j (c_s)_{l+1}^j \langle d_l^j|\hat{l}_-|d_{l+1}^j\rangle) \quad (9)$$

Here $(c_t)_k$ and $(c_s)_k$ are the atomic orbital (AO) coefficients in the half- and double-occupied HOMO in triplet and singlet states, respectively, retrieved from the DFT calculations on the system, d_k^j is the Pd atomic d orbitals, and superscript j enumerates palladium atoms. Equation 9 can be immediately used for the numerical estimations if we know the AO coefficients. With the neglect of the two-electron component, such calculations are expected to overestimate the transmission coefficient by a factor of ~1.5. This inaccuracy in the computation of the transmission coefficient is not crucial for our conclusions about reaction pathways.

Hydrogen Interactions with a Pd$_4$ Cluster

J. Phys. Chem. A, Vol. 105, No. 50, 2001 **11323**

Now, we are in a position to estimate the probability of the triplet−singlet transition for some approach modes of the considered reaction. Results of calculations on the reactants in the atom-to-face approach mode seem to be more appropriated for our purpose, because the saddle point has been localized in this case (see Figure 9). Substitution of numeral values for the corresponding AO coefficients at the saddle point into eq 9 and using the constant $\xi_{4d} = 1400$ cm^{-1} [45] gives the spin−orbit matrix element value $\sim$70 cm^{-1}. According to ref 38, the adiabaticity criterion of a chemical reaction V_{cr} might be approximately set as $k_B T = 208$ cm^{-1} at $T = 298$ K. It results in the transmission coefficient in eq 3 $\kappa = (V_{ts}/V_{cr})^2 \sim 0.1$; that is, the triplet−singlet transition probability in this approach mode is sufficiently high.

We managed to locate the saddle point along the bond-to-top reaction pathway (scheme **b** in Figure 1,i and PES cross-sections in Figure 3,ii). It appears to be feasible because of the close geometric structures of the triplet and singlet Pd$_4$H$_2$ complexes in the region of PES intersection (Figure 3,ii). So, the new triplet curve was calculated in the interval of x values between 1.8 and 2.4 Å, with the geometric parameters of the complex fixed at optimized values obtained for the singlet state. The crossing point between the singlet and the new triplet curves at $x = 2.27$ Å is where the structures and energies of the system are about the same in both of the spin states. This point is $\sim$20 kcal/mol higher in energy than the triplet reactants and represents an approximate estimation of the activation barrier for the considered approaching mode. The spin−orbit matrix element calculated in this point is $\sim$120 cm^{-1} and leads to the transmission coefficient $\kappa \sim 0.4$.

5. Discussion

On the basis of the analysis of the two-dimensional PES cross-sections[1−4] discussed in the Introduction, two mechanisms were suggested for hydrogen adsorption and dissociation on bulk palladium surfaces. The precursor mediated mechanism with molecular preadsorption state was supposed to prevail at the relatively low kinetic energy of the incident H$_2$ molecule, whereas the direct activated dissociation was expected for molecules approaching the surface with kinetic energy sufficient to overcome the activation barrier to dissociation. Hydrogen interactions with small palladium clusters studied by DFT methods for the flexible substrate geometry and allowed low symmetry[14,31] show essential distinctions with those obtained for the bulk surfaces. In this discussion, we analyze what features have to be attributed to the physical differences between bulk and cluster catalysts and to what extent the distinctions arise from the applied model approximations. For this aim, the energetics of hydrogen interactions with 1-, 2-, and 3-fold position (top, bond, and face, respectively) of the Pd$_4$ pyramid are compared with the resembling literature data for bulk surfaces and small clusters.

The end-on atom-to-top approach mode is unfavorable for interaction of a hydrogen molecule with palladium tetramer; the molecule tends to rotate into the side-on bond-to-top approach mode. The interaction between the Pd$_4$ cluster and H$_2$ molecule in this latter orientation is attractive at all distances between the reactants larger than 2 Å and leads to the formation of the weakly bound predissociated adsorption complexes (**A1**) and (**A0**) as it is shown in Figure 1,i. To the best of our knowledge, for bulk palladium surfaces, the former approach mode was not considered. The end-on hydrogen capture with formation of a weak linear Pd−H−H complex was assumed in the Pd−H$_2$ system.[24] However, frequency calculations[48] point out
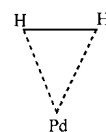
SCHEME 1

TABLE 3: Local Geometries and Stabilities of the Stable Predissociated Pd−H$_2$ Complexes Localized in the Side-on (Bond-to-Top) Approach Mode on Low Index Palladium Surfaces and Clusters[a]

substrate	ref	spin state	stability, kcal/mol[b]	geometry, Å		
				s	d	b
Pd(111)	1	singlet	4.9	1.74	0.84	0
Pd(100)	2	singlet	2.8	1.89	0.80	0
Pd(110)	4	singlet	8.8	1.80	0.80	0
Pd atom	31	singlet	19.4	1.63	0.88	
Pd$_3$	14	singlet	8.2	1.26	0.82	1.22
	14	triplet	10.9	1.41	0.81	1.13
Pd$_4$	14	singlet	9.9	1.46	0.79	1.13
	14	triplet	8.8	1.56	0.79	1.08
	present work	singlet	8.4	1.22	0.84	1.16
	present work	triplet	8.8	1.37	0.83	1.14

[a] See Figure 1,i for notations. [b] For the comparison purpose, the stabilities of the complexes are presented without zero-point corrections and with respect to the same spin state of reactants as that of the complexes.

that this configuration is not a real minimum, and forces again will turn it into the most stable in the system side-on orientation. The same is true for larger clusters. Nevertheless, this type of interaction presents the only case of small attraction between the palladium substrate and the incident hydrogen molecule if its molecular axis is oriented along the approach line.

The spontaneous formation of the molecular adsorption complex shown in the Scheme 1 was found in the side-on (bond-to-top) approach mode for all considered systems, namely, for low-index palladium surfaces[1−4] and for small clusters.[14,31] The local geometries and stabilities of such predissociated complexes are summarized in Table 3. In all structures except for the single palladium atom, the Pd−H distances are very close, the adsorbed hydrogen molecule is only slightly activated, and the geometry of the clusters is negligibly distorted by the adsorption. The stability of the molecular adsorption state on the clusters is somewhat higher than that on closely packed Pd (111) and (100) surfaces and is close to that on the crystallographically "open" Pd (110) plane. Therefore, the precursor state presents the most attractive position for the capping of a hydrogen molecule on bulk palladium surfaces and small clusters and precedes the hydrogen dissociation in both singlet and triplet states.

In the ground triplet state of the Pd$_4$−H$_2$ system, both atom-to-bond and bond-to-bond approach modes are characterized by repulsive interactions between the reactants in the entrance channel. At low kinetic energy, the incident hydrogen molecule is steered toward one of the palladium atoms of the attacked Pd−Pd bond with the formation of the molecular complex (**D1**) shown in Figure 4,ii. This final adsorption state has the same local structure as that shown in the Scheme 1 and is separated from the molecular complex (**A1**) by the activation barrier of about 2 kcal/mol. Similarly, in the excited singlet state, the interaction between the reactants is repulsive in both approach modes and the corresponding PES cross-sections do not involve any saddle point. These types of interactions do not lead to the hydrogen dissociation on Pd$_3$ cluster,[14] whereas a hydrogen molecule approaching the center of Pd$_2$ cluster with the molecular axis being perpendicular to the Pd−Pd bond dissoci-

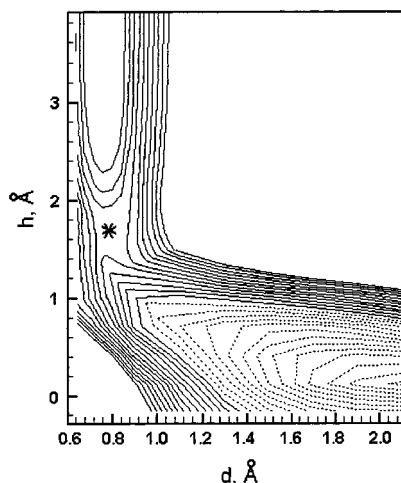**11324** *J. Phys. Chem. A, Vol. 105, No. 50, 2001*

German et al.

Figure 10. Two-dimensional PES for the perpendicular bond-to-bond approach of the hydrogen molecule toward the Pd$_4$ cluster with frozen geometry shown in Table 1 (scheme **a** in Figure 4,i).

ates spontaneously.[12] In the case of bulk palladium surfaces, the three-dimensional PES including an angular degree of freedom for H$_2$ approaching the 2-fold bridge position on the Pd (111) surface was considered in ref 7. The atom-to-bond approach mode was found to face an activation barrier of almost 2 eV. With allowed angular rotation the incident hydrogen molecule is bent to about 30° with the surface normal and reaches the mixed surface−subsurface final state overcoming two small activation barriers.

For the hydrogen molecule approaching low-index palladium surfaces with the molecular axis being parallel to the surface plane, the perpendicular bond-to-bond reaction pathway is believed to be the most favorable one leading to the dissociation without or with very low activation barrier[1−4,7]. Moreover, for the precursor mediated mechanism, it was suggested that the steering of the molecularly adsorbed hydrogen molecule from the 1-fold coordination position leads to its dissociation near the center of the Pd−Pd bond. To find out the source of such dramatic difference between infinite and cluster palladium particles, we applied the same method and model that were used for the modeling of hydrogen dissociation on low-index bulk surfaces[1−4] for the Pd$_4$−H$_2$ system in the singlet state. The two-dimensional "elbow" plot obtained for the frozen optimized structure of the Pd$_4$ cluster in C_{2v} symmetry (see Table 1) is shown in Figure 10. Qualitatively, this plot is very similar to those presented in refs 1−4 for the bulk surfaces and provides the activation barriers to dissociation of about 6.5 kcal/mol in comparison with 5.5 kcal/mol obtained for the relaxed cluster geometry (Figure 5,i). This barrier is significantly higher than that obtained for the same approach mode on the bulk surfaces. Such a behavior could be explained by the geometry of the coordination site. As it was shown earlier, the energy of the transition state to dissociation is in a great extent determined by the strength of the interaction between the σ^* orbital of H$_2$ and those of the substrate. The closer the hydrogen molecule has to approach the substrate for an effective filling of its σ^* MO, the higher the barrier to dissociation is. The transition state in the "elbow" plot in Figure 10 corresponds to the height of the hydrogen molecule 1.63 Å above the "surface" in comparison with 1.93 and 2.16 Å and corresponding barriers of 1.6 and 0.2 kcal/mol reported for Pd (111)[1] and Pd (100)[2], respectively.

Furthermore, as it was shown above, hydrogen dissociation does not occur within the adopted symmetry constraint and the

saddle point, which appears on the "elbow" plot, is characterized by several imaginary vibrations and thus does not presents the *real* transition state. This fact makes questionable the detailed mechanism of hydrogen dissociation on bulk surfaces on the basis of the 2D PES scan. As in the case of small palladium clusters, the hydrogen dissociation on bulk surfaces very likely proceeds via the pathway which is nonsymmetric one with respect to two hydrogen atoms described in detail for Pd$_3$ and Pd$_4$ clusters.[14] This reaction path involves the transition state to the dissociation, in which one of hydrogen atoms moves toward a bridge site and another one remains in the 1-fold position. In such a reaction pathway, the formation of predissociated complexes is of paramount importance, and this fact is consistent with the experimentally observed extremely high ratio of the molecular forms of hydrogen on palladium surfaces (67% on the dispersed Pd black[46]).

The atom-to-face and bond-to-face attack of hydrogen molecule toward the 3-fold position on the palladium tetramer is characterized by notable repulsion in the entrance channel. The only attractive interaction leads again to the formation of the molecular complexes with local structure shown in Scheme 1. The former approach mode was not considered for the hydrogen interaction with bulk palladium surfaces. The side-on hydrogen interaction with the 3-fold coordination site on the Pd (111) surface leading to the bridge-bridge final state faces a barrier of only 1.6 kcal/mol in the entrance channel of 2D PES.[1] The direct formation of more stable 3-fold-coordinated dissociated structures requires overcoming of two barriers of up to 3.2 kcal/mol. As in the previous case, the existence of the *real* transition states in these 2D surfaces was not proved.

The exceptional feature of hydrogen interaction with the Pd$_4$ cluster is that the ground state of reactants is a triplet, whereas the ground state of product is a singlet. It sets up the claim of the triplet−singlet transition along the reaction pathway. Detailed analysis of the singlet and triplet potential surfaces for the Pd$_4$−H$_2$ system indicates at least six possibilities for such a spin transition listed below:

1. Excitation of the palladium tetramer from the triplet to the singlet state located 16.5 kcal/mol higher and excitation of the triplet molecular complex (**A1**) to the singlet state (**A0**) (Figure 1,ii) leading to the 17.5 kcal/mol increase in energy. If the system reaches one of these two excited states, it will then follow along the reaction pathway presented in ref 14 for the singlet PES. This path includes an activation barrier to dissociation that is 8.8. kcal/mol lower in energy than the singlet reactants and only 4.2 kcal/mol above the precursor state. However, the probability of such a triplet−singlet transition includes the product of the matrix element of the spin−orbit operator, which admixes the disturbing wave function to the main spin state and the matrix element of the operator for interaction of a particle with electromagnetic field. Thus, such a transition is likely to be small as compared to that discussed in the previous section.

2. The triplet−singlet transition in the PES crossing points in the bond-to-top (scheme **b** in Figure 1,i and PES cross-sections in Figure 3,ii) and in the atom-to-face (scheme **d** in Figure 7,iii and PES cross-sections in Figure 9) reaction pathways. Estimations of the triplet−singlet transition probabilities show that the transition occurs by nonadiabatic mechanism with rather higher probability owing to a large constant of the spin−orbit coupling (1400 cm^{-1}). The corresponding transmission coefficients are ~0.4 and ~0.1 with the activation barriers to hydrogen dissociation of ~ 20 and ~ 25 kcal/mol, respectively. The former reaction path leads to the formation

Hydrogen Interactions with a Pd$_4$ Cluster

J. Phys. Chem. A, Vol. 105, No. 50, 2001 **11325**

of the dissociated Pd$_4$H$_2$ complex with hydrogen atoms located in 3-fold positions, whereas the latter path provides the transition state that transforms into the most stable in the system dissociated complex with hydrogen atoms in the most distant 2-fold positions. Other reaction modes considered in this work are supposed to have significantly higher activation energy. Additional crossing points between many-dimensional PESs, which correspond to Pd$_4$H$_2$ complexes with low symmetry, apparently exist and some of them could have lower energy and higher triplet−singlet transition probability.

3. The hydrogen dissociation in the triplet state followed by the radiant transition from the triplet complexes (**B1**) and (**F1**) to the corresponding singlet states (**B0**) and (**F0**) (Figures 1,ii and 4,iv and PES cross-sections in Figures 3,ii and 6,i, respectively). On the triplet PES, the reaction pathway for the dissociation involves the activation barrier of 2.8 kcal/mol with respect to the free reactants (10.5 kcal/mol with respect to the precursor state).[14] The following triplet−singlet transition seems to be more probable than that discussed in the first point owing to the reduction of the activation factor on the value of the radiation energy. Nevertheless, we suppose it is of the same order of smallness because of the diminutive admixing of the wave function with another multiplicity to the main spin state.

Therefore, we suppose that the radiative transitions are not effective in the hydrogen dissociation on small palladium clusters. The most probable way of the triplet−singlet transition seems to be via the saddle point on the intersection of the triplet and singlet potential surfaces. This conclusion is based on the approximate qualitative evaluation. For a more rigorous comparison of possible radiant spin transitions, the accurate estimate of the corresponding matrix elements is required.

6. Conclusions

In the present paper, we report the results of DFT study of the singlet and triplet PESs for hydrogen interactions with palladium tetramer. The energetics and dynamics of hydrogen interactions with 1-, 2-, and 3-fold position (top, bond, and face, respectively) of the Pd$_4$ pyramid are compared with the resembling literature data for bulk surfaces and small clusters. The main results of the present work may be summarized as follows:

1. The number of products with different spin states, geometric structures, and interaction energies could be formed in the system. The initial ground state of the system is triplet. In this spin state, several molecular complexes characterized by the binding energy of 5.3−6.2 kcal/mol and two dissociated complexes with binding energy of 4.7 and 8.4 kcal/mol are localized. Two dissociated singlet complexes characterized by the binding energy of 22.1 kcal/mol with hydrogen atoms sitting in the 3-fold and in the most distant 2-fold positions correspond to the ground state of the system. Several more local minima corresponding to the molecular and dissociated Pd$_4$H$_2$ complexes are localized in the singlet PES.

2. At low kinetic energy, the incident hydrogen molecule in any initial orientation is rotated and steered toward one of palladium atoms with spontaneous formation of the molecular complexes separated from each other by small barriers. The geometric structures of the Pd$_4$ and H$_2$ fragments are only slightly distorted in these complexes with respect to the free reagents. The local geometric structures of such complexes are very close to those reported for low-index bulk palladium surfaces; their stability is as high as that on the crystallographically "open" Pd (110) surface. This precursor state presents the most attractive position for the capping of a hydrogen molecule

on bulk palladium surfaces and small clusters far from the substrate and grants the only nonactivated channel for hydrogen interactions with small clusters.

3. Qualitatively, two-dimensional "elbow" plots for the hydrogen dissociation along the side-on bond-to-bond approach mode are very similar for the singlet Pd$_4$ cluster and for the single-crystal palladium surfaces with frozen optimized geometry. However, the activation barrier to the dissociation on the Pd$_4$ cluster of ∼6 kcal/mol is significantly higher than that on bulk surfaces. This difference is attributed to the geometric structure of the coordination site.

4. Detailed consideration of the singlet and triplet potential surfaces and analysis of the literature data[14] show that only one reaction pathway leading to the hydrogen dissociation exists on each PES. It proceeds via the precursor state as an intermediate and involves the nonsymmetric with respect to two hydrogen atoms transition state, in which one of the H atoms remains in the 1-fold coordination position and another one moves toward the nearest 2-fold site. The saddle point, which appears on the 2D "elbow" plot, is characterized by several imaginary vibrations and thus does not present the *real* transition state.

5. The two most favorable reaction pathways leading to the formation of the ground-state singlet dissociated structures from the ground-state triplet reactants involve the activation barriers of ∼20−25 kcal/mol. The system must surmount such an activation barrier in order to reach the crossing point between the triplet and singlet potential surfaces in which the spin transition becomes possible. The probability of the triplet− singlet transition is estimated to be in the range of ∼0.1−0.4. The radiative spin transitions in the system are supposed to have significantly lower probability.

6. Specific geometric and electronic structures of the Pd$_4$ cluster as compared to the bulk single-crystal surfaces result in the stabilization of the precursor state, in the increase of the activation barrier to hydrogen dissociation, and in the necessity of the triplet−singlet transition along the reaction pathway. As a sequence, the molecular adsorptive state of hydrogen is expected to be more pronounced on small palladium clusters than on the bulk surfaces.

References and Notes

(1) Dong, W.; Kresse, G.; Hafner, J. *J. Mol. Catal. A* **1997**, *119*, 69. Dong, W.; Hafner, J. *J. Phys. Rev. B* **1997**, *56*, 15396.

(2) Eichler, A.; Kresse, G.; Hafner, J. *Surf. Sci.* **1998**, *397*, 116.

(3) Wilke, S.; Scheffler, M. *Phys. Rev. B* **1996**, *53*, 4926.

(4) Ledentu, V.; Dong, W.; Sautet, P. *Surf. Sci.* **1998**, *412–413*, 518.

(5) Rendulic, K. D.; Anger, G.; Winkler, A. *Surf. Sci.* **1989**, *208*, 404. Resch, C.; Berger, H. F.; Rendulic, K. D.; Bertel, E. *Surf. Sci.* **1994**, *316*, L1105.

(6) Gdowski, G. E.; Stulen, R. H.; Felter, T. E. *J. Vac. Sci. Technol. A* **1987**, *5*, 1103.

(7) Løvvik O. M.; Olsen, R. A. *J. Chem. Phys*. **1996**, *104*, 4330. Olsen, R. A.; Philipsen, P. H. T.; Baerends, E. J.; Kroes, G. J.; Løvvik, O. M. *J. Chem. Phys*. **1997**, *106*, 9286. Olsen, R. A.; Kroes, G. J.; Baerends, E. J. *J. Chem. Phys*. **1998**, *109*, 2450. Olsen, R. A.; Kroes, G. J.; Løvvik, O. M.; Baerends, E. J. *J. Chem. Phys*. **1997**, *107*, 10652.

(8) Balasubramanian, K. *J. Chem. Phys*. **1988**, *89*, 6310.

(9) Balasubramanian, K. *J. Chem. Phys*. **1989**, *91*, 307.

(10) Dai, D.; Balasubramanian, K. *J. Chem. Phys*. **1995**, *103*, 648.

(11) Dai, D.; Balasubramanian, K. *Chem. Phys. Lett*. **1999**, *310*, 303.

(12) Cui, Q.; Musaev, D. G.; Morokuma, K. *J. Chem. Phys*. **1998**, *108*, 8418.

(13) Cui, Q.; Musaev, D. G.; Morokuma, K. *J. Phys. Chem*. **1998**, *102*, 6373.

(14) Moc, J.; Musaev, D. G.; Morokuma, K. *J. Phys. Chem. A* **2000**, *104*, 11606.

(15) Valerio, G.; Toulhoat, H. *J. Phys. Chem*. **1996**, *100*, 10827.

(16) Zacarias, A. G.; Castro, M.; M. Tour, M.; Seminario, J. M. *J. Phys. Chem. A* **1999**, *103*, 7692.

(17) Seminario, J. M.; Zacarias, A. G.; Castro, M. *Int. J. Quantum Chem*. **1997**, *61*, 515.

(18) Neurock, M.; van Santen, R. A. *J. Phys. Chem. B* **2000**, *104*, 11127.

(19) Harada, M.; Dexpert, H. *J. Phys. Chem*. **1996**, *100*, 565.

(20) Gatica, J. M.; Baker, R. T.; Fornasiero, P.; Bernal, S.; Kapar, J. *J. Phys. Chem. B* **2000**, *105*, 1191.

(21) Taniyama, T.; Ohta, E.; Sato, T. *Europhys. Lett*. **1997**, *38*, 195.

(22) van Leeuwen, D. A.; van Ruitenbeek, J. M.; Schmid, G.; de Jongh, L. J. *Physica B* **1994**, *194–196*, 263.

(23) Volokitin, Y.; Sinzig, J.; de Jongh, L. J.; Schmid, G.; Vargaftik, M. N.; Moiseev, I. I. *Nature* **1996**, *384*, 621.

(24) Novaro, O.; Jarque, C. *Theor. Chim. Acta* **1991**, *80*, 19.

(25) Siegbahn, P. E. M. *Theor. Chim. Acta*. **1994**, *87*, 441.

(26) Castillo, S.; Cruz, A.; Bertin, V.; Poulain, E.; Arellano, J. S.; Del Angel, G. *Int. J. Quantum Chem*. **1997**, *62*, 29.

(27) Nakatsuji, H.; Hada, M.; Yonezawa, T. *J. Am. Chem. Soc*. **1987**, *109*, 1902.

(28) Nakatsuji, H.; Hada, M. *J. Am. Chem. Soc*. **1985**, *107*, 8264.

(29) Balasubramanian, K.; Feng, P. Y.; Liao, M. Z. *J. Chem. Phys*. **1988**, *88*, 6955.

(30) Dai, D.; Liao, D. W.; Balasubramanian, K. *J. Chem. Phys*. **1995**, *102*, 7530.

(31) Efremenko, I.; German, E. D.; Sheintuch, M. *J. Phys. Chem*. **2000**, *104*, 8089.

(32) Frisch, M. J.; Trucks, G. W.; Schlegel, H. B.; Gill, P. M. W.; Johnson, B. G.; Robb, M. A.; Cheeseman, J. R.; Keith, T.; Petersson, G. A.; Montgomery, J. A.; Raghavachari, K.; Al-Laham, M. A.; Zakrzewski, V. G.; Ortiz, J. V.; Foresman, J. B.; Cioslowski, J.; Stefanov, B. B.; Nanayakkara, A.; Challacombe, M.; Peng, C. Y.; Ayala, P. Y.; Chen, W.; Wong, M. W.; Andres, J. L.; Replogle, E. S.; Gomperts, R.; Martin, R. L.; Fox, D. J.; Binkley, J. S.; Defrees, D. J.; Baker, J.; Stewart, J. P.; Head-Gordon, M.; Gonzalez, C.; Pople, J. A. *Gaussian 94*, revision A.1; Gaussian, Inc.: Pittsburgh, PA, 1995.

(33) Becke, A. D. *J. Chem. Phys*. **1993**, *98*, 5648.

(34) Lee, C.; Yang, W.; Parr, R. G. *Phys. Rev. B* **1988**, *37*, 785.

(35) Woon, D. E.; Dunning, T. H., Jr. *J. Chem. Phys*. **1993**, *98*, 1358.

(36) Hay, P. J.; Wadt, W. R. *J. Chem. Phys*. **1985**, *82*, 270, 299.

(37) Lide, D. R., Ed.; *Handbook of Chemistry and Physics*, 55th ed.; CRS Press: Boca Raton, FL, 1974–1975.

(38) Kuznetsov, A. M. *Charge transfer in Physics, Chemistry and Biology*; Gordon & Breach: Reading, U.K., 1995.

(39) Kuznetsov, A. M. *Stochastic and dynamic Views of Chemical Reaction Kinetics in Solutions*; Press politechnicues et universitaires romandes: Lausanne, Switzerland, 1999.

(40) King, H. F.; Furlani, T. R. *J. Comput. Chem*. **1988**, *9*, 771.

(41) Dewar, M. J. *The Molecular Orbital Theory of Organic Chemistry*; McGraw-Hill: New York, 1969.

(42) Castet, F.; Ducasse, L.; Fritsch, A. *Chem. Phys*. **1998**, *232*, 37.

(43) (a) Farazdel, A.; Dupius, M.; Clementy, E.; Aviram, A. *J. Am. Chem. Soc*. **1990**, *112*, 4206. (b) King, H. F.; Stanton, R. E.; Kim, H.; Wayatt, R. E.; Parr, R. G. *J. Chem. Phys*. **1967**, *47*, 1936.

(44) Carrington, A.; McLachlan, A. D. *Introduction to Magnetic Resonance*; Harper & Row: New York, 1967.

(45) Griffith, J. S. *The Theory of Transition-Metal Ions*, Cambridge University Press: New York, 1961.

(46) a) Babenkova, L. V.; Popova, N. M. *Kinet. Katal*. **1985**, *26*, 953 (in Russian). (b) Popova, N. M. *Katalit. Reaktsii v Zhidk. Faze*; Alma-Ata: Nauka, Russia, 1985; p 28–41 (in Russian).

(47) Fedorov, D. G.; Gordon, M. S. *J. Chem. Phys*. **2000**, *112*, 5611.

(48) Efremenko, I.; Sheintuch, M. Unpublished results.